

All-fiber, wavelength-tunable ultrafast praseodymium fiber laser

H. Ahmad^{1,2,*}, S. N. Aidit¹, S. I. Ooi¹, and Z. C. Tiu¹

¹Photonics Research Centre, University of Malaya, Kuala Lumpur, Malaysia

²Department of Physics, Faculty of Science and Technology, Airlangga University, Surabaya 60115, Indonesia

*Corresponding author: harith@um.edu.my

Received September 18, 2018; accepted November 1, 2018; posted online November 30, 2018

The interest in tunable ultrafast fiber lasers operating in the 1.3 μm region has seen a significant increase due to rising demands for bandwidth as well as the zero-dispersion characteristic of silica fibers in this wavelength region. In this work, a tunable mode-locked praseodymium-doped fluoride fiber (PDFF) laser using single-walled carbon nanotubes as a saturable absorber is demonstrated. The mode-locked pulses are generated at a central wavelength of 1302 nm with a pulse repetition rate of 5.92 MHz and pulse width of 1.13 ps. The tunability of the mode-locked PDFF laser covers a tuning range of 11 nm.

OCIS codes: 140.3510, 140.3600.

doi: 10.3788/COL201816.121405.

Ultrafast fiber lasers with tunable wavelength outputs have attracted substantial attention due to their applications in the areas of spectroscopy, biomedical diagnostics, material processing, and optical communications^[1-4]. Passively mode-locked fiber lasers are known to be economical, simple, and flexible sources of ultrafast pulses, and the incorporation of an optical filter as a tuning element in the laser cavity provides these lasers with significant potential for commercial applications.

Various passive mode-locking techniques have been explored in fiber lasers as a means to meet current demands for ultrafast signal sources in communication systems. Initially, mode locking in fiber lasers required the use of complex techniques or components, such as acousto- or electro-optical modulators^[5,6] and semiconductor saturable mirrors (SESAMs)^[3,7]. However, the complexity and fragility of these components made their use less than desirable. For instance, SESAMs are complex devices that are fabricated through the use of molecular beam epitaxy (MBE) in distributed Bragg reflectors (DBRs)^[8], and the optimization of their recovery time towards sub-picoseconds levels requires post growth ion implantation or low-temperature growth^[9]. As a result of this, significant research efforts have been made to develop materials that can serve as saturable absorbers (SAs) that are more cost effective to fabricate and easy to integrate into laser cavities, while at the same time achieving satisfactory mode-locking performance. The advent of low-dimensional materials provided a viable solution towards passively mode-locked fiber lasers, allowing for compact and cost-effective platforms to be realized.

In this regard, various low-dimensional materials, such as single-walled carbon nanotubes (SWCNTs)^[10-21], graphene^[22-28], and transition metal dichalcogenides (TMDs)^[29-37] have all demonstrated high potential to be used as SA materials. Among these materials, SWCNTs in particular have shown significant promise as low-

dimensional SA materials as a result of their simple synthesis process, short recovery time, high optical damage resistance, and wide absorption wavelength range. This is because SWCNTs are direct-bandgap materials, with a gap that is dependent on the diameter and chirality of the nanotube^[38]. Furthermore, SWCNTs exhibit large optical nonlinearity in the near-infrared region, making them advantageous for generating mode-locked outputs in fiber lasers within the 1.2 to 2.0 μm region^[39]. This would be a crucial development, as most SWCNT-based SA mode-locked fiber lasers are reported in the 1.0^[18,19], 1.5^[10-12,14-17,21], and 2.0 μm ^[20] regions, and few to none are reported in any other wavelength region. The shortest mode-locked pulse was obtained in the 1.5 μm region by Hou *et al.* with a pulse width of sub-200-fs in a dispersion-managed soliton ytterbium-doped fiber laser using an SWCNT-based SA^[18], while Popa *et al.* successfully demonstrated mode-locked pulses with a 74 fs width at 1.5 μm from a stretched-pulse laser with a SWCNT SA^[21]. Furthermore, SWCNT SAs have also been seen to be able to generate mode-locked outputs from a fiber laser in the 2.0 μm region with a pulse width as narrow as 450 fs, as reported by Chernysheva *et al.*^[20].

In conjunction with these developments, there has recently been renewed interest towards the generation of ultrafast pulses in the 1.3 μm wavelength region, also known as the O-band. The O-band is highly advantageous, as it allows for the zero dispersion of light propagating through a silica-based optical fiber^[40,41] and would thus be able to cater to the increasing demands for communication bandwidth. Operation in the O-band region is made possible through the use of praseodymium-doped fluoride fiber (PDFF), which is a reliable gain medium to induce lasing in the 1.3 μm region. The low phonon energy characteristics of the fluoride fiber host provides low non-radiative decay conditions, making the PDFF a highly desirable gain medium to generate an ultrafast phenomenon in

the 1.3 μm region^[42,43]. In this work, a tunable PDFFL using SWCNTs as an SA to induce mode locking is proposed and demonstrated. The proposed laser is designed to operate in the 1.3 μm region, with the ability to tune the generated output. The proposed laser would have significant applications, in particular, for communications systems.

The setup of the proposed tunable mode-locked PDFFL is given in Fig. 1. The laser cavity consists of a 11.7 m long PDFF, which serves as the gain medium. Fluoride glass with a $\text{ZrF}_4\text{-BaF}_2\text{-LaF}_3\text{-AlF}_3\text{-NaF}$ (ZBLAN) composition is used as a host glass for the praseodymium (Pr^{3+}) ions, as the low phonon energy characteristics of ZBLAN glass leads to low non-radiative decay and in turn greatly enhances emissions in the 1.3 μm region.

The PDFF with a Pr^{3+} concentration of 2.25×10^{-3} and an absorption coefficient of ~ 3 dB/m at 1020 nm is optically pumped with a 1020 nm laser diode (LD) using a 1020/1300 nm wavelength division multiplexer (WDM). An isolator (ISO) is incorporated in the setup to ensure the uni-directional propagation of light in the cavity, with the output port of the ISO connected to the SWCNT-based SA. The SA is formed by sandwiching the SWCNT film between two fiber ferrules using a fiber adaptor. The SWCNT used in this work is obtained from a previously prepared sample and has been described and characterized in detail in Ref. [44]. Figure 2 shows the nonlinear absorption curve of the SWCNT-based SA with a computed modulation depth of 18.6%, obtained with the balanced twin-detector method. The inset of the figure shows the Raman spectrum of the sample, with a sharp peak at 1549 cm^{-1} that corresponds to the G peak and confirms the presence of the carbon nanotubes in the SA. The SA has an insertion loss of around 3 dB at 1300 nm. A polarization controller (PC) connected to the output port of the SA assembly is

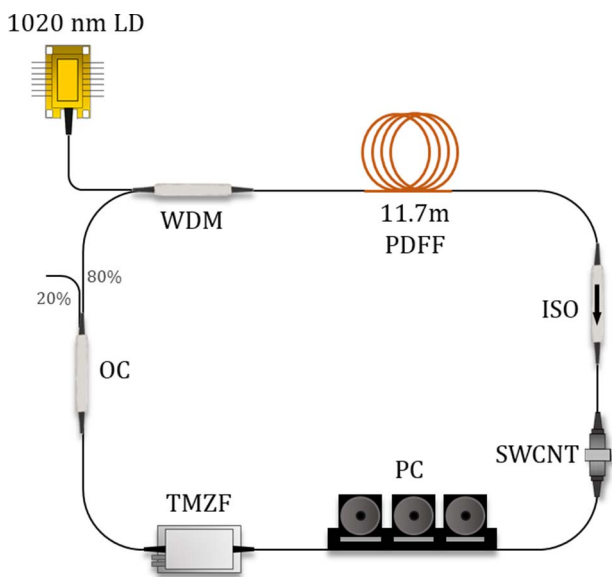


Fig. 1. Cavity setup of tunable mode-locked PDFFL.

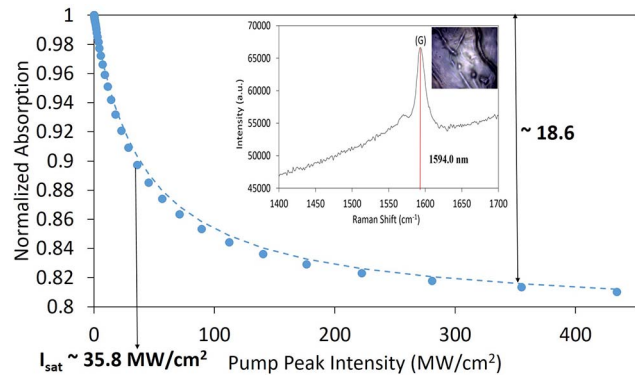


Fig. 2. Nonlinear absorption curve of the SWCNT SA. The inset shows the Raman spectrum. Reprinted with permission from Ref. [44], Science Press.

used to optimize the intra-cavity polarization state of the oscillating light, which is then channelled into a tunable Mach-Zehnder filter (TMZF), which serves as a wavelength tuning element. The TMZF has a tuning range of ~ 35 nm, a 3 dB bandwidth of 10 nm, and a maximum extinction ratio of ~ 26 dB in the 1.3 μm region. The filtered signal from the TMZF is connected to an 80:20 coupler, whereby 80% of the light is looped back to the 1300 nm port of the WDM, thus completing the optical cavity. The remaining 20% of the oscillating signal is extracted from the cavity for further analysis.

The total cavity length of the PDFFL is approximately 35.2 m, comprised of the 11.7 m long PDFF and approximately 23.5 m single-mode fiber (SMF-28). The PDFF group velocity dispersion (GVD) coefficient is $36\text{ ps}^2/\text{km}$, as provided in the official FiberLabs Inc. website, whereas the SMF-28 exhibits a GVD coefficient of $-1\text{ ps}^2/\text{km}$ at 1302 nm based on the SMF-28 dispersion curve. The net cavity dispersion of the proposed laser is thus calculated to be 0.398 ps^2 .

The generation of mode-locked pulses in the proposed fiber laser is first studied without the incorporation of the TMZF into the laser cavity. Under constant polarization, the proposed fiber laser experiences three different operation regimes under different pump powers: continuous-wave (CW), Q -switched mode locking (QML) and continuous-wave mode locking (CWML). The average output power from the laser at various stages against the incident pump power is plotted in Fig. 3. From the figure, it can be seen that the threshold incident pump power required to achieve CW operation is approximately 327 mW, and no pulsed behavior is observed until an incident pump power of 385 mW is reached. At this threshold power, the laser then switches to the QML regime and continues to operate in this mode until a pump power of 458 mW is attained. In the QML operation mode, the generated mode-locked pulse trains exhibit a fundamental frequency that tallies with the total cavity length and is modulated by the Q -switched pulse in the kilohertz region.

This confirms QML operation in the laser cavity, which then evolves into CWML operation as the incident pump

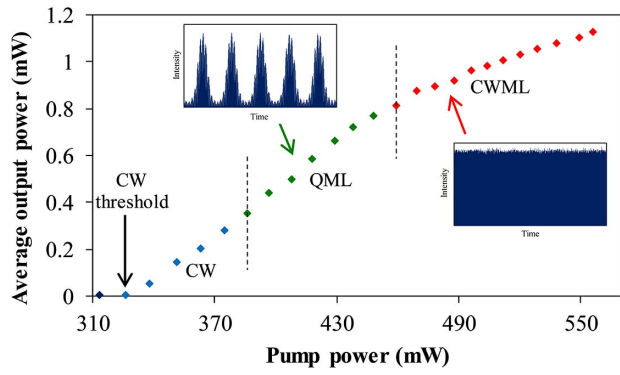


Fig. 3. Average output power against pump power. Different marker color represents different laser operation. The inset shows the oscilloscope trace of QML and CWML operations.

power reaches 459 mW. CWML operation is sustained up to the maximum pump power of 556 mW, corresponding to the maximum average output power of 1.13 mW, but it is limited in the proposed laser by the availability of higher pump powers from the 1020 nm LD. In the CWML regime, mode-locking operation is achieved at a threshold pump power of 459 mW, with stable mode-locking operation observed for pump powers ranging between 459 and 556 mW.

Figure 4 depicts the characteristics of the mode-locked PDFFL at pump power of 556 mW. As the different spectral components move at different speeds, the output characteristics of the mode-locked fiber laser are strongly affected by intra-cavity dispersion^[37,45,46]. Both the PDFFL and SMF have positive and negative GVDs of 36 ps²/km and -1 ps²/km, respectively, giving a net cavity dispersion of 0.398 ps² and resulting in mode-locking operation in the stretched-pulse regime. This is validated by the smooth and broad Gaussian-like spectrum that is typical of stretched-pulse lasers, as given in Fig. 4(a)^[11,47,48]. The optical spectrum is obtained with a Yokogawa

AQ6370B optical spectrum analyser (OSA) and observed at 1302 nm with a 3 dB bandwidth of 2.3 nm. The mode-locked pulse train is given in inset (I) of Fig. 4(a) and can be seen to exhibit a repetition rate of 5.92 MHz with a pulse-to-pulse interval of 169 ns, correlating to the cavity roundtrip time. The mode-locked pulse is detected with a Newport 818-BB-35 F 12.5 GHz photodetector with a responsivity of 0.77 A/W at 1300 nm in conjunction with a 500 MHz Yokogawa DLM2054 oscilloscope with a sampling rate of 2.5 GS/s. Inset (II) of Fig. 4(a) depicts the autocorrelation trace with a pulse width of 1.13 ps based on a Gaussian fitting profile. The achievable pulse width of the passively mode-locked fiber laser is strongly influenced by the gain bandwidth, cavity length, and nonlinearities in the laser cavity, as well as the specific characteristics of the SA, such as its modulation depth^[49–51]. The time-bandwidth product is calculated to be approximately 0.46, which is slightly higher than the transform limit of 0.44 and is indicative of a low chirping in the cavity. Measurement of the RF spectra of the generated pulses is given in Fig. 4(b) and shows a high intensity peak at 5.92 MHz, auguring well with the fundamental frequency of the cavity. The signal-to-noise ratio (SNR) is measured to be ~ 60 dB, indicating a highly stable mode-locked pulse with low timing jitter. Furthermore, no other spectrum modulation is observed over a larger 500 MHz frequency span, as depicted in inset (I) of Fig. 4(b), further indicating that only a single pulse has been generated. The maximum output power of the mode-locked pulse is measured to be 1.13 mW, corresponding to pulse energy of 191 pJ.

The stability of the pulsed laser's operation is further evaluated by monitoring the mode-locked spectra over a period of 60 min at intervals of 10 min. It can be seen that the mode-locked spectrum is stable with no significant degradation observed at any point, as shown in inset (II) of Fig. 4(b). It can be seen that the central wavelength and spectral width of the spectrum remain constant over

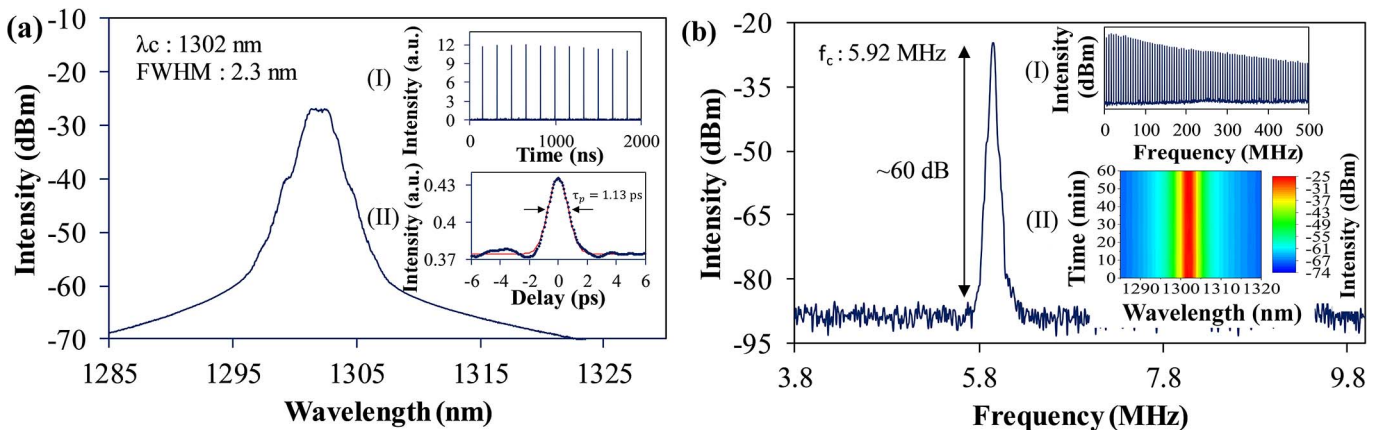


Fig. 4. Characteristics of mode-locked PDFFL at pump power of 556 mW. (a) Optical spectrum [inset (I), pulse train and (II), autocorrelation trace (dotted line) with Gaussian fit (solid line)] and (b) RF spectrum. Inset (I) shows the RF spectrum with a 500 MHz span and (II) gives the optical spectrum stability of the mode-locking operation over a period of 1 h.

the entire test period, indicating that the pulsed O-band output operates very well under typical operating conditions.

Tunability in the mode-locked PDFFL is achieved by incorporating the TMZF into the laser cavity. The incorporation of the TMZF allows for the central wavelength of the mode-locked output to be tuned from 1296 to 1307 nm. The full-width at half-maximum (FWHM) of the PDFFL's amplified spontaneous emission (ASE) spectrum covers a range of 1290 to 1319 nm. Thus, the lasing wavelength range of the PDFFL will be constrained towards this wavelength region. Figure 5 shows the mode-locked output spectra at a pump power of 556 mW for different central wavelengths achieved by adjusting the TMZF. As seen from the figure, the 3 dB spectral bandwidth of the spectrum experiences a variation of $\sim 20\%$ against the shift of the central wavelength. The change in the FWHM spectral bandwidth is almost certainly due to light propagating through silica fiber that experiences different dispersions under different operating wavelengths.

The demand for ultrafast fiber lasers at different operating wavelengths has long been an issue of concern by the industry and, thus, been the focus of significant research efforts. To date, numerous materials and rare-earth-doped fibers have been employed as SAs and gain media to generate ultrashort pulses in different wavelength regions. Figure 6 provides an overview of ultrafast fiber lasers with pulse widths at different operating wavelengths utilizing SWCNTs^[10–21], graphene^[22–28], and TMDs^[29–37] as SAs. As can be seen from the figure, the generation of mode-locked fiber lasers has been intensively focused on operating in the 1.0^[18,19,23,24,32,34,36], 1.5^[10–12,14–17,21,24–28,31–33,35,37], and 2.0 μm regions^[13,20,22,26,29,30] through the use of ytterbium-, erbium-, and thulium-doped fibers, respectively, as gain media. However, limited efforts have been made to investigate mode-locked generation in the 1.3 μm region. Among the first few demonstrations of a passively mode-locked fiber laser operating in the 1.3 μm region

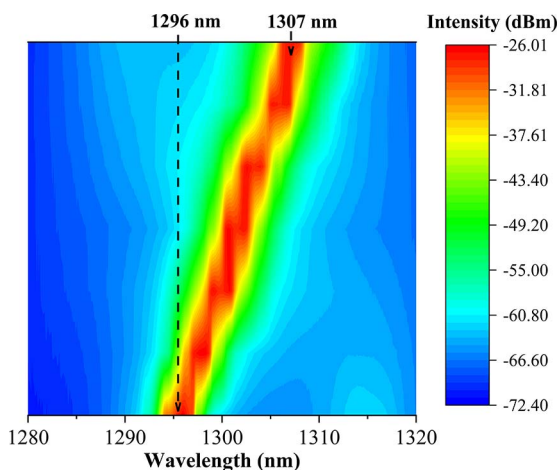


Fig. 5. Mode-locked output spectra at different central wavelengths with the incorporation of a tunable Mach–Zehnder filter, covering a tuning range of 11 nm.

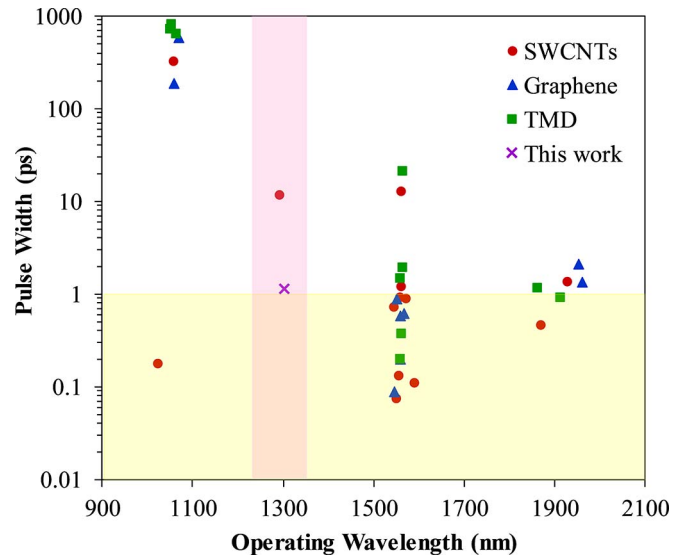


Fig. 6. Overview of mode-locked fiber lasers using different low-dimensional material SAs, which are classified in terms of operating wavelength and pulse width.

was reported by Song *et al.* in 2005 with a minimum pulse width of 11.6 ps^[52]. In this work, a pulse width of 1.13 ps is achieved, which indicates a significant improvement over previous works, and it can be said with high certainty that the shorter pulse width is almost certainly due to the all-fiber configuration of the proposed laser. Furthermore, the proposed laser is also able to achieve mode locking with a repetition rate of 5.92 MHz, which is slightly higher than that reported by Song *et al.* at 3.18 MHz. Contrary to achievements in the 1.0, 1.5, and 2.0 μm regions, the pulse width of the 1.3 μm fiber laser is still considered broad, as it is limited in the picosecond pulse width. This is mainly constrained by the long length of the PDFFL gain medium, as well as higher power loss of fluoride soft glass in the 1.3 μm region, as compared to the loss profile of silica in other wavelength ranges.

In this work, tunable mode-locked pulses are generated from a proposed PDFFL using an SWCNT-based SA, as experimentally demonstrated in this work. The all-fiberized and compact PDFFL delivers pulses at 1302 nm with a pulse width of 1.13 ps and produces a mode-locked pulse train at 5.92 MHz with pulse energy of 191 pJ. The central wavelength of the laser can be continuously tuned with the incorporation of TMZF, covering a tuning range of 11 nm. To the best of the author's knowledge, these are the shortest mode-locked pulses and the first tunable mode-locked pulses obtained from PDFFL so far.

This work was supported by the Ministry of Higher Education, Malaysia under the grants LRGS (2015) NGOD/UM/KPT and GA010-2014 (ULUNG) and the University of Malaya under the grant RU 001-2017.

References

1. V. S. Letokhov, *Nature* **316**, 325 (1985).
2. U. Keller, *Nature* **424**, 831 (2003).

3. O. Okhotnikov, A. Grudinin, and M. Pessa, *New J. Phys.* **6**, 177 (2004).
4. K. Sugioka and Y. Cheng, *Light Sci. Appl.* **3**, e149 (2014).
5. D. D. Hudson, K. W. Holman, R. J. Jones, S. T. Cundiff, J. Ye, and D. J. Jones, *Opt. Lett.* **30**, 2948 (2005).
6. M. Y. Jeon, H. K. Lee, K. H. Kim, E. H. Lee, W. Y. Oh, B. Y. Kim, H. W. Lee, and Y. W. Koh, *Opt. Commun.* **149**, 312 (1998).
7. U. Keller, K. J. Weingarten, F. X. Kärtner, D. Kopf, B. Braun, I. D. Jung, R. Fluck, C. Höminger, N. Matuschek, and J. Aus Der Au, *IEEE J. Sel. Top. Quantum Electron.* **2**, 435 (1996).
8. O. G. Okhotnikov, T. Jouhti, J. Konttinen, S. Karirinne, and M. Pessa, *Opt. Lett.* **28**, 364 (2003).
9. U. Keller and R. Paschotta, *Ultrafast Lasers* (CRC Press, 2002).
10. F. Wang, A. G. Rozhin, V. Scardaci, Z. Sun, F. Hennrich, I. H. White, W. I. Milne, and A. C. Ferrari, *Nat. Nanotechnol.* **3**, 738 (2008).
11. Z. Sun, T. Hasan, F. Wang, A. G. Rozhin, I. H. White, and A. C. Ferrari, *Nano Res.* **3**, 404 (2010).
12. S. Yamashita, Y. Inoue, S. Maruyama, Y. Murakami, H. Yaguchi, M. Jablonski, and S. Y. Set, *Opt. Lett.* **29**, 1581 (2004).
13. M. A. Solodyankin, E. D. Obraztsova, A. S. Lobach, A. I. Chernov, A. V. Tausenev, V. I. Konov, and E. M. Dianov, *Opt. Lett.* **33**, 1336 (2008).
14. I. Hernandez-Romano, D. Mandridis, D. A. May-Arrijo, J. J. Sanchez-Mondragon, and P. J. Delfyett, *Opt. Lett.* **36**, 2122 (2011).
15. C. Zou, T. Wang, Z. Yan, Q. Huang, M. AlAraimi, A. Rozhin, and C. Mou, *Opt. Commun.* **406**, 151 (2018).
16. H. Jeong, S. Y. Choi, F. Rotermund, Y.-H. Cha, D.-Y. Jeong, and D.-I. Yeom, *Opt. Express* **22**, 22667 (2014).
17. W. S. Kwon, H. Lee, J. H. Kim, J. Choi, K.-S. Kim, and S. Kim, *Opt. Express* **23**, 7779 (2015).
18. L. Hou, H. Guo, Y. Wang, J. Sun, Q. Lin, Y. Bai, and J. Bai, *Opt. Express* **26**, 9063 (2018).
19. X. Li, Y. Wang, Y. Wang, W. Zhao, X. Yu, Z. Sun, X. Cheng, X. Yu, Y. Zhang, and Q. J. Wang, *Opt. Express* **22**, 17227 (2014).
20. M. A. Chernysheva, A. A. Krylov, P. G. Kryukov, N. R. Arutyunyan, A. S. Pozharov, E. D. Obraztsova, and E. M. Dianov, *Opt. Express* **20**, B124 (2012).
21. D. Popa, Z. Sun, T. Hasan, W. B. Cho, F. Wang, F. Torrisi, and A. C. Ferrari, *Appl. Phys. Lett.* **101**, (2012).
22. Q. Wang, T. Chen, B. Zhang, M. Li, Y. Lu, and K. P. Chen, *Appl. Phys. Lett.* **102**, 131117 (2013).
23. L. M. Zhao, D. Y. Tang, H. Zhang, X. Wu, Q. Bao, and K. P. Loh, *Opt. Lett.* **35**, 3622 (2010).
24. H.-R. Chen, C.-Y. Tsai, H.-M. Cheng, K.-H. Lin, and W.-F. Hsieh, *Opt. Express* **22**, 12880 (2014).
25. J. Xu, J. Liu, S. Wu, Q.-H. Yang, and P. Wang, *Opt. Express* **20**, 15474 (2012).
26. J. Boguslawski, J. Sotor, G. Sobon, R. Kozinski, K. Librant, J. Tarka, L. Lipinska, and K. M. Abramski, *Photon. Res.* **3**, 119 (2015).
27. J. Sotor, I. Pasternak, A. Krajewska, W. Strupinski, and G. Sobon, *Opt. Express* **23**, 27503 (2015).
28. B. Fu, Y. Hua, X. Xiao, H. Zhu, Z. Sun, and C. Yang, *IEEE J. Sel. Top. Quantum Electron.* **20**, (2014).
29. J. Lee, J. Koo, J. Lee, Y. M. Jhon, and J. H. Lee, *Opt. Mater. Express* **7**, 2968 (2017).
30. J. Wang, W. Lu, J. Li, H. Chen, Z. Jiang, J. Wang, W. Zhang, M. Zhang, I. Ling Li, Z. Xu, W. Liu, and P. Yan, *IEEE J. Sel. Top. Quantum Electron.* **24**, (2018).
31. E. J. Aiub, D. Steinberg, E. A. Thoroh De Souza, and L. A. M. Saito, *Opt. Express* **25**, 10546 (2017).
32. D. Mao, S. Zhang, Y. Wang, X. Gan, W. Zhang, T. Mei, Y. Wang, Y. Wang, H. Zeng, and J. Zhao, *Opt. Express* **23**, 27509 (2015).
33. R. Khazaeinezhad, S. H. Kassani, H. Jeong, K. J. Park, B. Y. Kim, D.-I. Yeom, and K. Oh, *IEEE Photon. Technol. Lett.* **27**, 1581 (2015).
34. L. Li, S. Z. Jiang, Y. G. Wang, X. Wang, L. N. Duan, D. Mao, Z. Li, B. Y. Man, and J. H. Si, *Opt. Express* **23**, 28698 (2015).
35. Z. Luo, Y. Li, M. Zhong, Y. Huang, X. Wan, J. Peng, and J. Weng, *Photon. Res.* **3**, A79 (2015).
36. H. Zhang, S. B. Lu, J. Zheng, J. Du, S. C. Wen, D. Y. Tang, and K. P. Loh, *Opt. Express* **22**, 7249 (2014).
37. Y. Cui, F. Lu, and X. Liu, *Sci. Rep.* **7**, 40080 (2017).
38. H. Kataura, Y. Kumazawa, Y. Maniwa, I. Umezumi, S. Suzuki, Y. Ohtsuka, and Y. Achiba, *Synth. Met.* **103**, 2555 (1999).
39. T. Hasan, Z. Sun, F. Wang, F. Bonaccorso, P. H. Tan, A. G. Rozhin, and A. C. Ferrari, *Adv. Mater.* **21**, 3874 (2009).
40. H. Onaka, H. Miyata, G. Ishikawa, K. Otsuka, H. Ooi, Y. Kai, S. Kinoshita, M. Seino, H. Nishimoto, and T. Chikama, in *Optical Fiber Communication Conference*, Optical Society of America (1996), paper PD19.
41. K. Mukasa, Y. Akasaka, Y. Suzuki, and T. Kamiya, in *11th International Conference on Integrated Optics and Optical Fibre Communications, and 23rd European Conference on Optical Communications (IET, 1997)*, p. 127.
42. Y. Ohishi, E. Snitzer, G. H. Sigel, T. Kanamori, T. Kitagawa, and S. Takahashi, *Opt. Lett.* **16**, 1747 (1991).
43. M. Yamada, M. Shimizu, T. Kanamori, Y. Ohishi, Y. Terunuma, K. Oikawa, H. Yoshinaga, K. Kikushima, Y. Miyamoto, and S. Sudo, *IEEE Photon. Technol. Lett.* **7**, 869 (1995).
44. H. Ahmad, S. A. Reduan, A. Z. Zulkifli, and Z. C. Tiu, *Appl. Opt.* **56**, 3841 (2017).
45. Y. Cui and X. Liu, *Opt. Express* **21**, 18969 (2013).
46. X. Liu, X. Yao, and Y. Cui, *Phys. Rev. Lett.* **121**, 23905 (2018).
47. Y. Wang, S. Alam, E. D. Obraztsova, A. S. Pozharov, S. Y. Set, and S. Yamashita, *Opt. Lett.* **41**, 3864 (2016).
48. K. Krzempek, G. Sobon, P. Kaczmarek, and K. M. Abramski, *Laser Phys. Lett.* **10**, 105103 (2013).
49. H. Jeong, S. Y. Choi, F. Rotermund, and D.-I. Yeom, *Opt. Express* **21**, 27011 (2013).
50. Q. Wang, J. Geng, T. Luo, and S. Jiang, *Opt. Lett.* **34**, 3616 (2009).
51. A. Chong, H. Liu, B. Nie, B. G. Bale, S. Wabnitz, W. H. Renninger, M. Dantus, and F. W. Wise, *Opt. Express* **20**, 14213 (2012).
52. Y. W. Song, S. Y. Set, S. Yamashita, C. S. Goh, and T. Kotake, *IEEE Photon. Technol. Lett.* **17**, 1623 (2005).